IEEE Robotics and Automation Letters (RA-L) paper, presented at ICRA 2026, Vienna, Austria. Cite as RA-L paper.

A Versatile Underactuated Robotic Hand for Cloth Manipulation

Xinhao Chen, Alberto Elías Petrilli Barceló, *Member, IEEE*, Shiry Ghidary Saeed, Dayuan Chen, *Member, IEEE*, Jose Victorio Salazar Luces, and Yasuhisa Hirata, *Member, IEEE*

***Abstract*—Traditional cloth manipulationg often employs low-DOF grippers to simplify hardware. However, this approach presents significant challenges for algorithms due to the complex and dynamic behavior of fabrics. To address these limitations, we propose a novel approach based on a human-hand-like design that integrates an underactuated grasping mechanism with a suction system. By incorporating multiple single-layer suction principles, the robotic hand achieves greater adaptability and flexibility, enabling it to perform tasks that would typically require high-DOF hands and complex control strategies. This letter outlines the design of the robot hand with a suction system and evaluates its performance in various tasks.**

***Index Terms*—Development and prototyping, industrial robots, product design.**

I. Introduction

IN RECENT years, with the rapid advancement of robotics technology and the growing advantages of automation, more industries are actively adopting robotic systems. In various applications, the core workflow typically follows a perception-decision-execution process.

First, as an essential component of the perception stage,vision systems, especially computer vision, have developed to a level sufficient to support complex automated sorting and grasping tasks, eliminating the need for traditional mechanical positioning or manual operations [1]. Deep learning plays a key role in this development. Compared to earlier vision methods that relied on handcrafted features (such as edge detection or color histograms), deep learning automatically extracts features from large datasets, greatly improving the performance of image recognition, object detection, and semantic segmentation [2], [3]. Second, the application of reinforcement learning in the decision-making stage is becoming increasingly widespread. Through extensive training in simulated environments, robots can autonomously learn manipulation strategies and transfer them to real-world environments, adapting to complex situations such as manipulation in contact [4], unknown objects [5], dynamic environments [6], and human-robot collaboration [7]. The core of the execution stage—the robotic hand—has long been a major research focus. Traditional industry has favored simple-structured, in recent years, underactuated robotic hands have gradually become mainstream [8], [9]. These hands feature passive compliance in their fingers, enabling them to conform to objects of various shapes. They offer advantages such as structural simplicity, ease of control, and high adaptability, without requiring additional actuators.

Despite ongoing advances in object manipulation technologies, grasping deformable objects (such as fabrics) remains a challenge. Their stretchability and softness lead to diverse and unpredictable shapes, making it difficult for robots to perform stable and efficient automated tasks. Current research primarily focuses on the development of recognition algorithms, often paired with simple one-degree-of-freedom grippers or underactuated hands designed for rigid objects [10], [11], [12]. However, when dealing with fabrics that are inherently compliant, underactuated fingers often provide only basic functionality, resulting in complex recognition and control algorithms. To simplify the control process, some studies have focused on developing task-specific robotic hands [13], [14], [15]. These specialized grippers maintain low cost and simple control without increasing the number of actuators and significantly reduce the reliance on recognition and control algorithms. However, such dedicated mechanisms still lack versatility when faced with multi-task switching scenarios.

To address this limitation, We have redefined the versatility of robotic hands and, based on this concept, designed a versatile robotic hand specifically for textiles previously [16]. Building on this, we added new features and redesigned a robotic hand (Fig. 1). The following sections are organized as follows: Section II defines the concept of versatility in this context; Section III details the proposed mechanism and analyses its gripping force; Section IV presents experiments demonstrating the gripper's capabilities; Section V concludes the letter and outlines future work.

II. Concept of Versatile Hand for Garment

The concept of a versatile hand for garments differs from that of a gripper for rigid objects. While grippers for rigid objects can grasp items of various shapes by passively deforming their fingers, soft objects like clothes are more challenging to handle. They deform unpredictably and may conform to the shape of

Received 4 January 2025; accepted 22 July 2025. Date of publication 11 August 2025; date of current version 27 August 2025. This article was recommended for publication by Associate Editor W. Jong Yoon and Editor H. Moon upon evaluation of the reviewers' comments. This work was supported by the Innovation and Technology Commission of the HKSAR Government under the InnoHK initiative. *(Corresponding author: Xinhao Chen.)*

The authors are with the Department of Robotics, Graduate School of Engineering, Tohoku University, Sendai 980-8579, Japan (e-mail: chen.xinhao.s1@dc.tohoku.ac.jp; hirata@srd.mech.tohoku.ac.jp).

This article has supplementary downloadable material available at https://doi.org/10.1109/LRA.2025.3597486, provided by the authors.

Digital Object Identifier 10.1109/LRA.2025.3597486

IEEE Robotics and Automation Letters (RA-L) paper, presented at ICRA 2026, Vienna, Austria. Cite as RA-L paper.

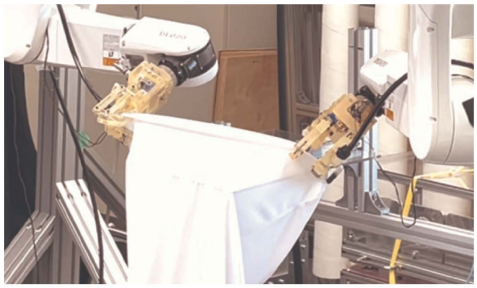

(a) Task execution (setting the T-shirt on the plate).

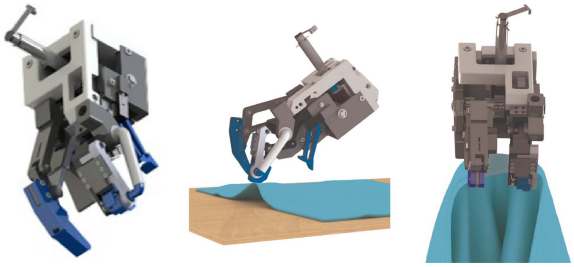

(b) Appearance. (c) Single-layer suction. (d) Linear grasp.

Fig. 1. Versatile robot hand for garment handling.

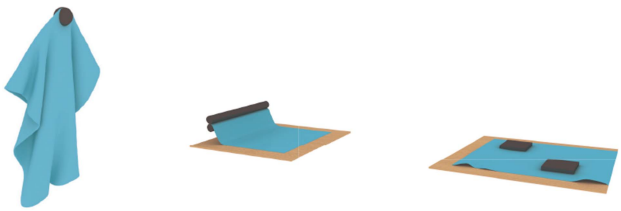

(a) Point Gripping. (b) Linear Gripping. (c) Plane Gripping.

Fig. 2. For textiles, it is possible to characterize most of the grasp using only three geometric entities points, lines and planes.

the fingers or environment. As a result, robot hands designed for rigid objects often only perform basic functions like clamping when handling garments. Versatility in this context refers to the hand's ability to perform a range of tasks with the same piece of clothing. Two key factors in garment manipulation are the shape of the fingertips and the trajectory of the fingertip (grasping principle).

Most grasps for garments rely on three geometric entities: points, lines, and planes (see Fig. 2) [17]. Point contact offers the smallest controlled area, suitable for precise grasping at specific locations like edges, corners, or wrinkles [18]. However, extensive contact may trap nearby wrinkles, impacting subsequent tasks. Conversely, line or plane contact provides larger controlled areas, facilitating better control and stability. For tasks like folding or sewing, line or plane contact is preferred due to their ability to control larger fabric areas and apply even pressure.

To enhance versatility, robot hands should accommodate various contact shapes, akin to human hands. Grippers are categorized based on gripping principles such as mechanical gripping, or using pins, brushes, vacuums, air jets, electrostatic, or adhesive methods (Fig. 10). Clamp grippers, commonly used

(a) Mechanical gripping. (b) Vacuum suction.

Fig. 3. Various methods to grasp flat-lying clothes.(a) Utilizing mechanical fingers to grasp flat-lying clothes (b) Employing suction pad to lift flat-lying clothes.

for picking and placing tasks [19], [20], offer a simple mechanical structure and firm grasp but may struggle with flat lying clothes or separation tasks. In contrast, needle, brush, vacuum, air jets, electrostatic, and adhesive grippers require only one side for gripping, enhancing efficiency in tasks like separating items from a stack [21], [22]. However, caution is needed with needle grippers to avoid fabric damage, while electrostatic grippers raise security concerns due to high voltage requirements [21].

Vacuum-based grippers face limitations due to the air permeability of clothes and weak tangential force, resulting in less firm grasping compared to clamp grippers, especially under external force or when interacting with other objects. On the other hand, adhesive grippers typically consist of belts and/or rollers covered with glue, but this method can affect fabric quality and cause functional issues in subsequent processing tasks [21].

Recognizing these limitations, integrating multiple grasping principles into a robot hand enables it to tackle various tasks and mitigate drawbacks associated with individual methods. Therefore, we proposed a robot hand that possess the following characteristics:

1) Incorporate two types of contact (point and linear contact).
2) Employ multiple grasping principles or motions for coordinated work.
3) Use fewer motors to reduce costs and simplify control.

III. Features of the Proposed Mechanism

In order to explain and test the functionality of the proposed robotics hand we are going to use the T-shirt production process as example, specifically focusing on the printing task. This process involves handling T-shirts from a stack, placing them onto the printing machine, executing the printing, and then removing them. Initially, clothing states can be broadly categorized into two: neatly and flatly stacked or scattered on the table or in a box. Let's first address the scenario where clothes are neatly stacked. In this case, several tasks need to be addressed:

1) Removing the top single piece of clothing while ensuring the grasping point is on a single layer of fabric.
2) Finding an appropriate grasping point and deforming the clothing to fit the board.
3) Adjusting the clothing's position and posture on the plate to minimize wrinkles.
4) After printing, removing the clothing from the plate.

Tasks 1 and 4 primarily require point grasping, while tasks 2 and 3 may necessitate line grasping or even plane contact. Task 1, involving grabbing the top piece of clothing, benefits from single-sided contact due to its nature. Task 2 requires

IEEE Robotics and Automation Letters (RA-L) paper, presented at ICRA 2026, Vienna, Austria. Cite as RA-L paper.

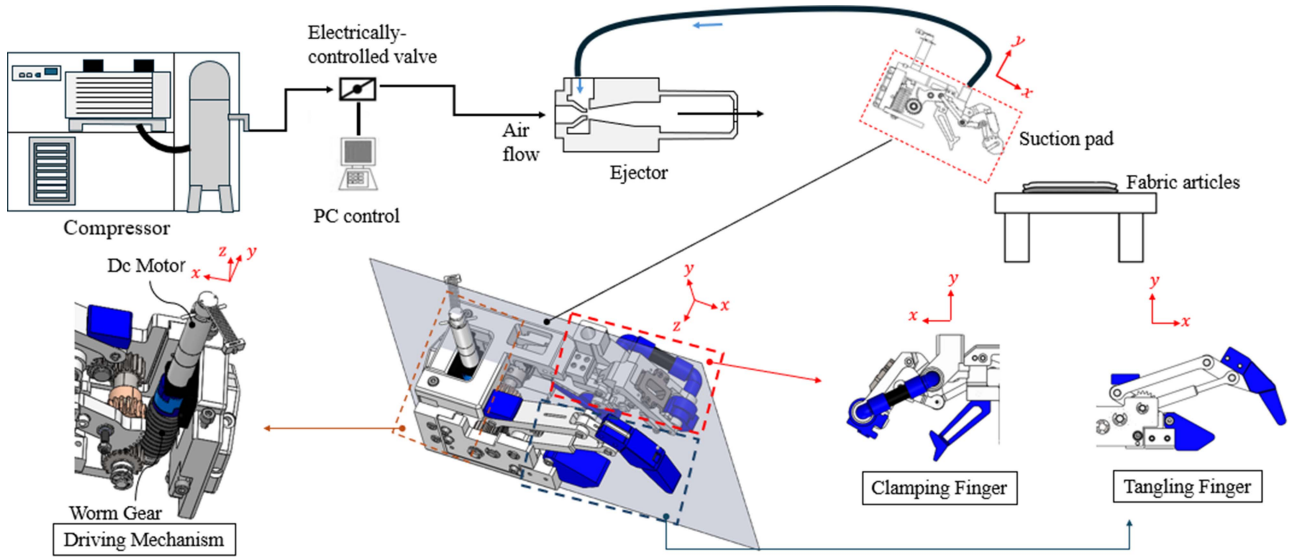

Fig. 4. Diagram of the suction system and robot hand structure.

overcoming resistance from the board and tensile force, necessitating two-sided contact to prevent slipping. Furthermore, depending on the shape of the board, there may be a need to transition from point contact to line contact. In Task 3, the plate size greatly affects how easily the garment can be set. A narrow plate makes sliding the garment easier but can cause misalignment and wrinkles. A wider plate makes placement harder but helps the garment stretch out, improving accuracy.

Therefore, our robotic hand must be capable of both point grasping and linear grasping. The grasping strategies and principles to be implemented should include single and two-sided contact grasping, as well as the transition from point contact to line contact. For efficiency and safety reasons, we opted for vacuum suction to perform single-sided contact grasping and combine it with clamp motion for a firm grip. As shown in the Fig. 4, our gripping system consists of suction system and robotic hand. The robotic hand is composed of a clamping finger, a tangle finger, and a driving mechanism.

A. *Vacuum System*

The vacuum system consists of a compressor, an electrically controlled valve, a vacuum generator ejector, and a suction pad (Fig. 4). Due to the air permeability of clothing, a high-suction-flow vacuum generator is essential to achieve the necessary pad pressure.

As it is essential to avoid removing two items of clothing from a pile at the same time. In the context of suction systems the primary cause of dual-pickup is the significant suction flow rate, which generates a vacuum between the second and first piece of clothing. To address this challenge, we adopted two methods: 1) Drawing up single fabric edge by suction, as shown in Fig. 5; 2) Adjusting the vacuum level approach for single-suction.

1) Drawing up Single Fabric Edge by Suction: By pressing down on the fabric edges, we prevent unwanted friction and sliding between layers during suction (Fig. 5). The suction force

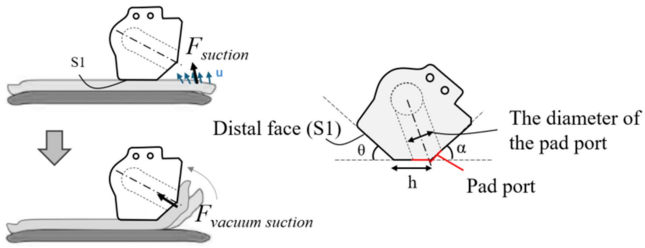

Fig. 5. Drawing up single fabric edge by suction.

results from airflow velocity changes on the fabric's surface, which reduces static pressure and creates a pressure difference, lifting the fabric. The suction force can be expressed as:

$$F_{\text{suction}} = \iint_S \frac{\rho}{2} u(x,y)^2 \, dx \, dy \tag{1}$$

Here, $u(x,y)$, S, and ρ represent the air velocity, the surface area of the fabric subject to suction force, and density of the air. When the fabric is drawn into the pad port, a quasi-closed space forms, enhancing suction proportional to the pad port's area:

$$F_{\text{vacuum suction}} = A_e \times P_{pad} \tag{2}$$

Where A_e, P_{pad}, represent the effective contact area of vacuum suction range, suction pad negative pressure respectively.

Suction performance depends on pad positioning and geometry, including the angle θ between surface $S1$ and the fabric, pad port diameter, distance h from the port center to surface $S1$, and angle α (Fig. 5). The pad port's diameter should ensure sufficient suction force ($F_{\text{vacuum suction}}$) for subsequent operations, while other parameters are tuned for effective single-layer suction.

2) Adjusting the Vacuum Level Approach for Single-Suction: By introducing a deliberate leakage point near the suction pad, the vacuum level and suction force can be controlled to ensure only a single fabric layer is suctioned. After separation, the leakage point can be sealed using a solenoid valve or similar

IEEE Robotics and Automation Letters (RA-L) paper, presented at ICRA 2026, Vienna, Austria. Cite as RA-L paper.

mechanism to restore full suction force. In the experiment, the leakage tube's inner diameter was fixed at 7 mm for ease of adjustment via its length.

The pressure inside the suction pad follows the ideal gas law:

$$PV = nR_{\text{air}}T, \tag{3}$$

where:

- P is the absolute pressure inside the suction pad.
- V is the volume from the vacuum generator to the suction port.
- n is the amount of gas (in moles).
- R_{air} is the specific gas constant for air.
- T is the temperature.

The vacuum generator evacuates a volume V of air in time Δt, where:

$$V = Q_c \Delta t, \tag{4}$$

and Q_c is its maximum suction flow rate under standard conditions. Leakage arises from the fabric, intentional design, and unknown causes, contributing Q_L, Q_{CL}, and Q_x, respectively, to the total air influx:

$$(Q_L + Q_{CL} + Q_x)\Delta t. \tag{5}$$

Using the ideal gas law, the pressure can be expressed as:

$$P = \frac{(Q_L + Q_{CL} + Q_x)R_{\text{air}}T}{V_m \cdot Q_c}, \tag{6}$$

where V_m is the molar gas volume. At maximum vacuum pressure P_1 (achieved when $Q_L = Q_{CL} = 0$), the leakage flow rate Q_x is givenby:

$$Q_x = \frac{P_1}{P_0} Q_c, \tag{7}$$

where P_0 is atmospheric pressure. For fabric leakage Q_L, related to material properties, we have:

$$Q_L = \frac{(P_L - P_1)}{P_0} Q_c, \tag{8}$$

where P_L is the pressure when there is no intentional leakage. Substituting these relationships into the ideal gas law, the final equation becomes:

$$\frac{\left(C_1 + \frac{C_2}{L}\right) P_0^2 + P_1 Q_c}{Q_c + (C_1 + \frac{C_2}{L})P_0} - P_0 = P_{\text{pad}} \tag{9}$$

where:

- L is the leakage tube length,
- P_{pad} is suction pad negative pressure,
- C_1, C_2 represents the leakage conductance of pad and intentional design.

B. Clamping Finger

Integrating the suction function into the 1-degree-of-freedom (1-DOF) fingertip can sometimes result in a discrepancy between the suction and clamping surfaces due to the limited DOF of the finger. This mismatch may cause incomplete clamping or outright failure. To address this issue, we introduce an underactuated structure in this section. As the input link rotates, the pad will adjust its angle relative to the output link to ensure consistency and prevent discrepancies. We conduct analysis of the underactuated mechanism and examine the gripping force.

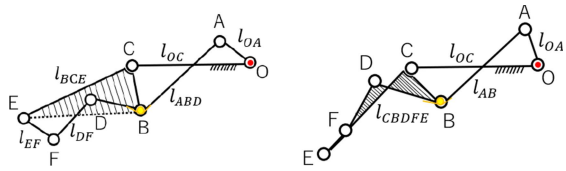

(a) Motion 1. (b) Motion 2.

Fig. 6. Proposed underactuated mechanism of clamping finger.(a)six-bar linkage in motion 1 (b)four-bar linkage in motion 2.

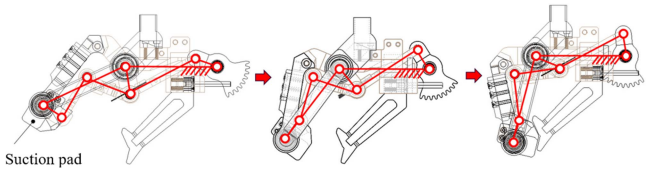

Fig. 7. Motion of underactuated finger.

1) The Underactuated Motion of the Clamping Finger: As illustrated in Fig. 6, the proposed underactuated mechanism includes a spring and stopper at joint B to restrict the movement of links AB and BD during finger actuation. A suction pad is integrated into link EF.

The mechanism's motion is divided into two stages, as depicted in Fig. 6. In the first stage (referred to as motion 1), the mechanism functions as a six-bar linkage composed of link OA, link OC (a fixed link), link ABD (with displacement restricted by the spring), link BCE, link DF, and link EF. Due to the presence of the spring, the upper links BD and AB rotate around joint A as a single unit, driven by the motion of link OA. Meanwhile, links CE, BC, and EJ (which carries the suction pad) rotate around joints C and E, respectively, until link EF comes into contact with the stopper (Fig. 6(a)). In the subsequent stage (referred to as motion 2), links EF, DF, BCE, and BD combine to function as a single unified link, simplifying the mechanism into a four-bar linkage. This motion enables the mechanism to clamp the clothes after adjusting the position of the suction pad installed on link EF (Fig. 6(b)). The continuous motion sequence of clamping finger is illustrated in the Fig. 7.

2) Analysis of the Gripping Force: By placing the mechanism (motion 2) in the XY plane (as shown in Fig. 8), the angle θ_{xx} is defined as the counterclockwise angle between link xx and the global X-axis. Applying the principle of virtual power to action 2, we obtain:

$$\boldsymbol{T}_{\text{in}} \cdot \dot{\boldsymbol{\theta}}_{OA} - k\Delta\theta \cdot \dot{\theta}_B = \boldsymbol{T}_{\text{out}} \cdot \dot{\boldsymbol{\theta}}_{CB} \tag{10}$$

where k represents the spring constant, T_{in} refers to the torque applied by the driving source at joint O, while T_{out} represents the torque transmitted to joint C, $\Delta\theta$ represents the angular variation of angle $\angle ABD$ in motion 2, which occurs due to the deformation of the spring located between links AB and BD.

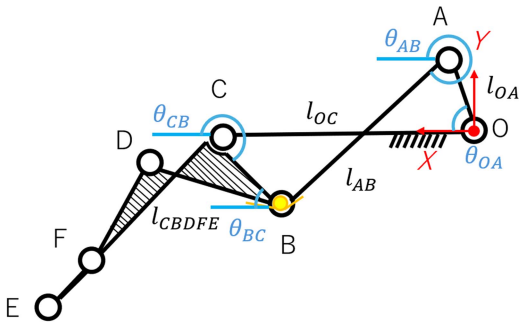

Fig. 8. Mechanism diagram placed in the complex plane (θ_{xx} is defined as the counterclockwise angle between link xx and the global X-axis).

Thus, we get:

$$\dot{\theta}_B = \angle C\dot{B}A = \dot{\theta}_{AB} - \dot{\theta}_{BC} \tag{11}$$

Differentiating the closed-loop equation of linkage O-A-B-C with respect to time, we get:

$$i\vec{OA}\dot{\theta}_{OA} - i\vec{AB}\dot{\theta}_{AB} - i\vec{BC}\dot{\theta}_{BC} = 0 \tag{12}$$

By dividing (12) into real and imaginary parts and solving the simultaneous linear equations, the relationship between $\dot{\theta}_{OA}$, $\dot{\theta}_{AB}$, and $\dot{\theta}_{BC}$ is derived as:

$$\begin{aligned}\dot{\theta}_{AB} &= \frac{\overline{OA}}{\overline{AB}}\frac{\sin(\theta_{BC}-\theta_{OA})}{\sin(\theta_{BC}-\theta_{AB})}\dot{\theta}_{OA} = \alpha\dot{\theta}_{OA} \\ \dot{\theta}_{BC} &= \frac{\overline{OA}}{\overline{BC}}\frac{\sin(\theta_{AB}-\theta_{OA})}{\sin(\theta_{AB}-\theta_{BC})}\dot{\theta}_{OA} = \beta\dot{\theta}_{OA}\end{aligned} \tag{13}$$

By substituting the above equations into ((10)), T_{out} is denoted as:

$$T_{\text{out}} = \frac{T_{\text{in}} - (\alpha-\beta)k\Delta\theta}{\beta} \tag{14}$$

Then, the grip force f on the contact point is derived as:

$$f = \frac{T_{\text{out}}}{l} \tag{15}$$

where l represents the distance from the axis of rotation to the line of action of force f.

3) Details of the Clamping Finger Design: Due to the breathability of the clothing, a certain tube diameter is required to maintain a sufficient suction cup pressure by ensuring adequate airflow. However, a larger tube diameter may obstruct the movement of the fingers. To address this issue, a special design is implemented (Fig. 10): the tube near the suction pad passes through the rotation axis, preventing deformation or twisting of the tube during finger movements.

C. Tangling Finger

Before positioning the cloth onto the plate, the width of the board becomes critical. If the plate is wide, the cloth needs to stretch to match its shape. During this stretching process, the size of the contact area with the cloth significantly influences the outcome. A larger contact area (resembling line-type contact) ensures uniform stretching of the fabric, thereby forming a fixed

Fig. 9. Trajectory of the tangling finger.

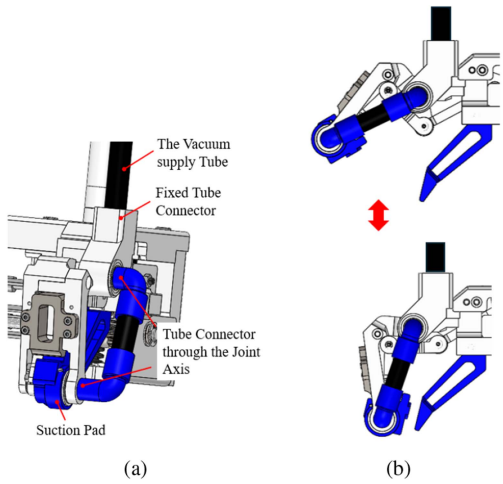

Fig. 10. Air tube integration in the finger mechanism to avoid obstruction and deformation. (a) Details of the clamping finger design. (b) No tube deformation during finger closure.

rectangular shape. In contrast, a smaller contact area (resembling point-type contact) may cause the shape to shrink, particularly taking on a parabolic shape due to insufficient tension and the pronounced effect of gravity. This uneven force distribution increases the likelihood of fabric deformation, potentially causing the fabric to become stuck during the setting process due to an irregular shape or an excessively narrow entrance.

To address this issue, the robotic hand should be capable of switching from point contact to line contact. This is the precise function of the tangling finger, allowing for a change in the contact area to control a larger portion of the fabric, facilitating the achievement of the desired shape. This action is not only necessary for inserting into the printing board but also for other tasks such as hanging clothes on hangers or fitting onto a human body model. However, due to the soft material of clothing, it is easily influenced by gravity and the environment, leading to deformation and increasing the difficulty of the switching motion.

Hence, it is essential to adjust the trajectory of the 2nd fingertip or the position and posture of the robot hand to ensure successful cloth gripping and avoid failure. This necessitates a redesign of the finger mechanism to achieve the desired trajectory. For instance, the tangling finger can extend and tangle the clothes, as depicted in Fig. 9. Fig. 11 describes the proposed mechanism and motion, utilizing a simple four-bar underactuated driving structure, where one of the bars AB is connected to bar BC through a spring. As the driving component (bar OA) rotates, fingertip D rotates around center O. When bar BA hits the

IEEE Robotics and Automation Letters (RA-L) paper, presented at ICRA 2026, Vienna, Austria. Cite as RA-L paper.

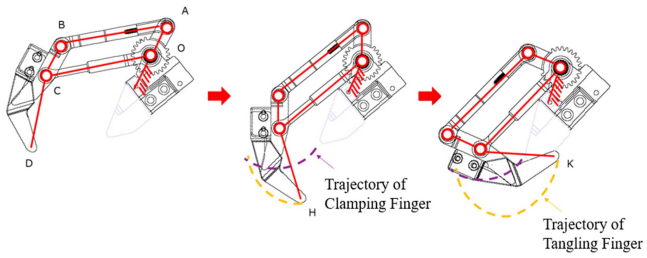

Fig. 11. Underactuated structure of the tangling finger.

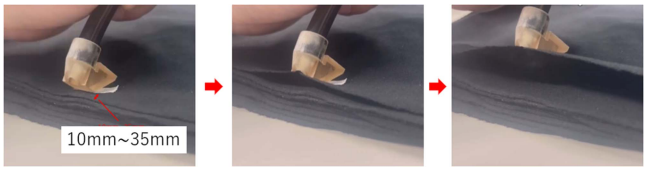

Fig. 12. Experiment of Drawing up single fabric edge by suction (suction of a single layer of fabric from a pile, with the fabric material being cotton and a thickness of 0.5 mm).

stopper, the rotation center of the fingertip changes from point O to point C, moving along the trajectory passing through points H and K, where H represents the grasping point and K denotes the finger closure point.

D. Driving Mechanism

Fig. 4 illustrates the driving mechanism of the developed robot hand. The DC motor's power is transmitted through a worm wheel to two worm gears, which subsequently rotate the gear links of the two fingers via a gear train.

IV. Experimental Results

To evaluate the efficiency of the developed robot hand, a series of experiments were conducted. First, standalone suction pad tests assessed the performance, advantages, and limitations of the two proposed methods. Then, grasping and setting tests were performed using the robotic arm.

A. Experiments on Single-Layer Suction With Two Methods

To validate two different approaches for single-layer fabric suction—specifically, the single fabric edge method and the vacuum-level adjustment method—we conducted comparative experiments under identical conditions. To assess the positional tolerance of the first method and compare its performance with the second, the hem of the garment was laid flat to ensure alignment of the upper and lower fabric layers. The suction pad was positioned vertically above the hem area. In the first method, the surface S1 of the pad was kept parallel to the fabric layer(Fig. 12); In the second method, the pad port was placed in direct contact with the fabric surface (Fig. 14). The vertical distance between the pad and the fabric edge was set to 10 mm $\sim$ 35mm.

The experimental equipment had the following parameters: The vacuum generator achieved a pressure of -81 kPa, with a

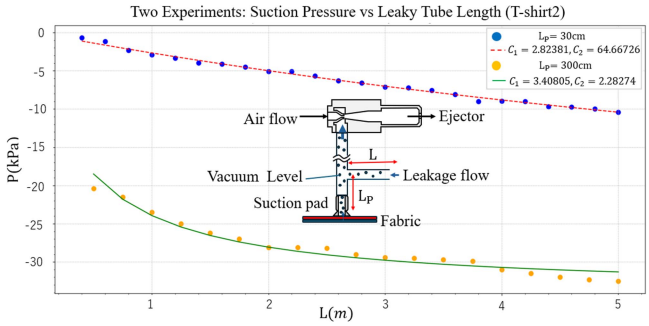

Fig. 13. Experiment on the relationship between leakage tube length L and suction pad negative Pressure P_{pad} (the distance L_P between the leakage tube and the suction pad is fixed at 30 cm and 300 cm, fitted curve is (9)).

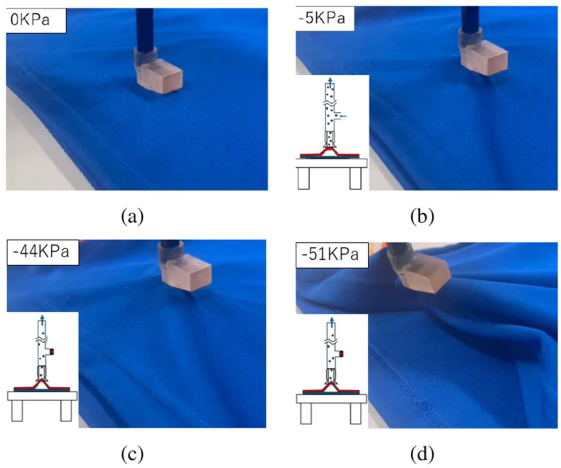

Fig. 14. Experiment of single-suction by adjusting the vacuum Level. (a) Position the suction pad vertically inside the garment. (b) Open the compressed air solenoid valve and leakage valve to pick up a single fabric layer. (c) Close the leakage valve after separating the first layer. (d) As the fabric deforms, the suction pad becomes sealed, further strengthening the suction.

suction flow rate of $225\,\mathrm{L/min}$ (ANR); the output pressure of the vacuum compressor ranged from 0.7 MPa to 0.8 MPa. The inner diameter of the vacuum pipeline was 7 mm, and the suction pad parameters included an opening angle of $\theta = 30°$, height $h = 9$ mm, pad port diameter of 4 mm, and port inclination angle $\alpha = 37°$. In the second suction method, the length of the leakage tube (L) was 2 meters, and its distance from the suction pad (L_P) was fixed at 0.3 meters.

At each position, 20 consecutive picking attempts were performed, and a successful single-layer pick was regarded as a success. This experiment tested various fabric materials and thicknesses, with detailed experimental results and fabric parameters summarized in Table I, the breathability was determined according to (8), and the T/B ratio is defined as the fabric thickness divided by the breathability. Additionally, for T-shirt 2, we collected pressure values related to the length of the leaky tube, with L_P set to 30 cm, and 3 m, and fitted the conductivity parameters C_1 and C_2. The experimental results and parameters are shown in Fig. 13.

Based on the experimental results, the first method performed well for fabrics with high T/B values (>2), but its success rate

TABLE I
RESULT OF EXPERIMENT A

Object	Material	Hem Thickness	Fabric Thickness	Breathability	T/B	SSR(10mm)		SSR(15mm)		SSR(20mm)		SSR(25mm)		SSR(30mm)		SSR(35mm)	
						M1	M2	M1	M2	M1	M2	M1	M2	M1	M2	M1	M2
T-shirt1	Polyester100%	1.4mm	0.7mm	51.24L/min	1.4	✓	✓	✓	✓	✓	✓	✓	✓	19/20	✓	14/20	✓
T-shirt2	Polyester100%	0.8mm	0.4mm	64.2L/min	0.62	19/20	✓	18/20	✓	✓	✓	✓	✓	6/20	✓	2/20	✓
T-shirt3	Cotton100%	2mm	1mm	44.5L/min	2.24	✓	✓	✓	✓	✓	✓	✓	✓	✓	✓	✓	✓
T-shirt4	Cotton100%	1.4mm	0.7mm	33.41L/min	2.09	✓	✓	✓	✓	✓	✓	✓	✓	✓	✓	✓	✓
Y-shirt5	Linen100%	-	0.5mm	35.64L/min	1.40	✓	✓	✓	✓	✓	✓	18/20	✓	16/20	✓	14/20	✓
T-shirt6	Cotton64%, Polyester36%	1.4mm	0.7mm	42.44L/min	1.65	✓	✓	✓	✓	✓	✓	✓	✓	✓	✓	6/20	✓
Y-shirt7	Cotton40%, Polyester40%	-	0.5mm	24.5L/min	2.04	✓	✓	✓	✓	✓	✓	✓	✓	✓	✓	✓	✓
T-shirt8	Polyester70%, Nylon30%	1mm	0.5mm	51.24L/min	0.98	✓	✓	✓	✓	✓	✓	6/20	✓	2/20	✓	0/20	✓
T-shirt9	Nylon85%Polyester15%	0.6mm	0.3mm	69.06L/min	0.43	12/20	✓	12/20	✓	14/20	✓	2/20	✓	0/20	✓	0/20	✓

SSR(xxmm) means suction success rate at xx mm distance from the hem. M1 and M2 represent Method 1 and Method 2 for single-layer suction
✓ means 20/20, T/B ratio is defined as fabric thickness divided by breathability.

TABLE II
RESULT OF EXPERIMENTS

Experiment	Object	Suction Method	Successes
Experiment B(1)	T-shirt1	Adjusting vacuum level	20/20
Experiment B(2)	T-shirt3	Drawing up fabric edge	18/20
Experiment B(3)	T-shirt3	-	10/10

declined as the T/B value decreased. Fabrics with T/B < 1 tend to be thinner, lighter, and more breathable, which makes single-layer separation more challenging. In contrast, for the second method, as the distance between the leak tube and the suction pad increased, the leakage tube conductivity C_2 decreased relative to the the fabric conductivity parameter C_1. This indicates that the leakage tube's influence on internal pressure weakens with distance (Fig. 13). Leveraging this principle, the system can flexibly handle a wide range of garment types with varying fabric properties. As a result, even for fabrics with low T/B values, the second method still achieves a high success rate. However, this approach requires additional control equipment, leading to a more complex system design.

B. Experiments on Single-Layer Grasping and Setting Tasks

To evaluate the performance of the developed robotic hand in handling single-layer fabrics, we designed a series of experiments with two primary objectives: (i) to verify whether the robotic hand can effectively transition from single-layer suction separation to mechanical grasping for setting onto the target when using different suction methods; (ii) to assess the necessity and effectiveness of employing linear grasping when setting onto the target with widths similar to the garments. The clothing dimensions were 490 mm in width and 650 mm in length. Two types of plates were used: a plastic plate (300 mm width, 400 mm length, 5 mm thickness) and a wooden plate (450mm width, 680 mm length, 20 mm thickness).

1) Picking and Setting by Adjusting the Vacuum Level: A series of experiments were conducted to assess the capability of the robotic hand to pick up a T-shirt from the top layer and place it onto a plastic plate. In this experiment, the grasping points were located on the first layer of fabric of the t-shirt. Initially, the top layer of the T-shirt was suctioned and grasped, and then placed onto the plastic plate as depicted in Fig. 15. As shown in Table II, this experiment used the method of adjusting the vacuum level of the suction pad to achieve single-layer suction. A series of 20 consecutive experiments was conducted, all of which were successful.

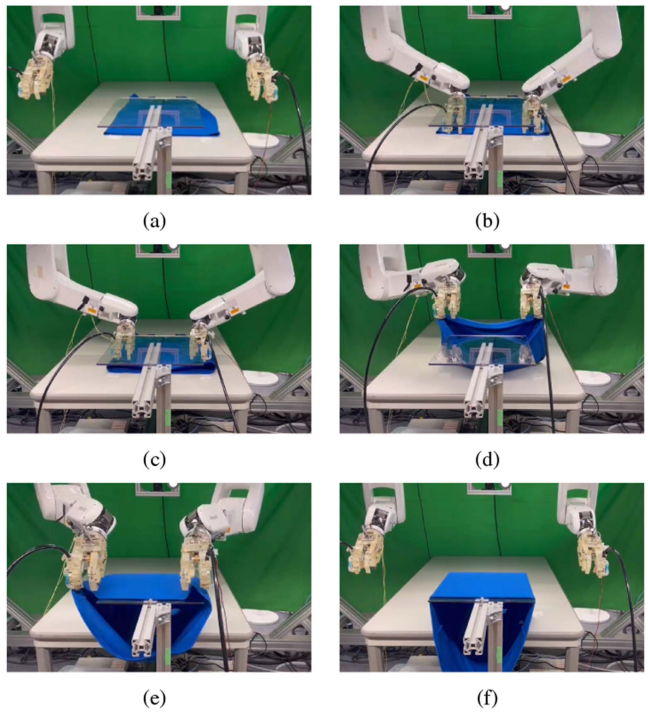

Fig. 15. Picking up from the top layer and setting experiment.

2) Picking and Setting by Drawing up the Fabric Edge: This set of experiments employed the edge suction method, with suction points fixed at a distance of 10–20 cm from the hem. The experimental results are shown in Table II, the reason for the experiment failure is that the ungrasped edges of the clothing sometimes get caught on the plastic board during movement, causing the setting to fail. Moreover, this method is sensitive to positional errors, particularly in the vertical direction; excessive errors may lead to garment deformation or curling, bringing the fabric too close to the suction pad. Therefore, a force sensor is required to regulate the applied force on the garment. In addition, localization errors from the recognition system can also affect the success rate for certain garments. In comparison, the vacuum-level adjustment method exhibits greater robustness to these errors.

3) Linear Grasping With Tangling Finger: Following the evaluation of the first finger, the functionality of the second finger (tangling finger) to generate Linear Grasp was tested. Initially, insertion onto the narrow plastic plate was straightforward. Subsequently, experiments were conducted using a larger wooden

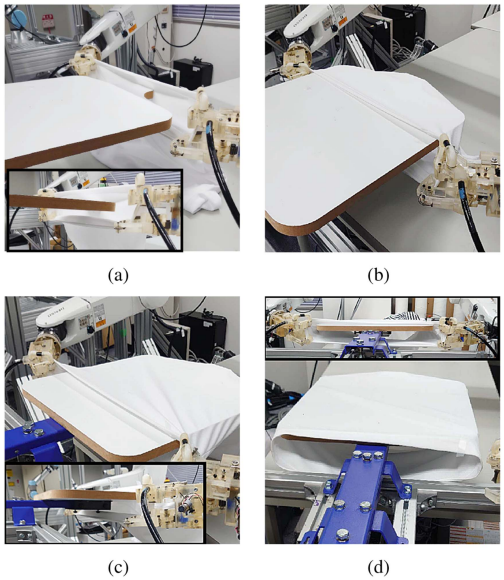

Fig. 16. Setting experiment of switching from point grasping to Linear grasping.

plate, where point grasp is not enough to achieve successfully the task. Subsequently, setting experiments using line grasping were conducted with the procedure outlined in Fig. 16. When employing linear grasping for insertion, the opening width and length were considerably larger than the wooden plate, facilitating smooth placement. As shown in Table II, the experiment was conducted 10 times, and all attempts were successful. This is because the shape of the garment was fixed during the insertion process, preventing uncontrolled sections from getting stuck on the plate.

V. Conclusion and Future Directions

In this study, we have developed a specialized robotic hand tailored for garment handling. This innovative underactuated robotic hand integrates suction capabilities with mechanical grasping features and demonstrates the flexibility to switch between point and linear contact as needed for various tasks. Through experiments, we summarized the advantages and disadvantages of the two methods. In future work, we will attempt to develop a smarter suction mechanism that can adjust strategies based on suction results, such as detecting single-layer, double-layer, or suction failure scenarios, and adjusting actions accordingly, such as aborting the current operation and retrying the suction. At the same time, we will make improvements to the mechanism design to accommodate more diverse actions and principles, increasing versatility while maintaining the advantages of fewer motors and low cost, and even making further optimizations.

References

[1] Z. Dong et al., "PPR-Net: Point-wise pose regression network for instance segmentation and 6D pose estimation in bin-picking scenarios," in *Proc. IEEE/RSJ Int. Conf. Intell. Robots Syst.*, 2019, pp. 1773–1780.

[2] C.-Y. Wang, A. Bochkovskiy, and H.-Y. M. Liao, "YOLOv7: Trainable Bag-of-Freebies sets new State-of-the-Art for real-time object detectors," in *Proc. IEEE/CVF Conf. Comput. Vis. Pattern Recognit.*, Vancouver, BC, Canada, 2023, pp. 7464–7475.

[3] Y. Li et al., "MViTv2: Improved multiscale vision transformers for classification and detection," in *Proc. IEEE/CVF Conf. Comput. Vis. Pattern Recognit.*, New Orleans, LA, USA, 2022, pp. 4794–4804.

[4] Y. Zhang, D. Chen, W. He, A. E. Petrilli Barceló, J. V. Salazar Luces, and Y. Hirata, "Multi-critic reinforcement learning for garment handling: Addressing unpredictability in temporal-phase continuous contact tasks," *IEEE Trans. Automat. Sci. Eng.*, vol. 22, pp. 10741–10752, 2025.

[5] X. Zhao, W. Liang, X. Zhang, C. M. Chew, and Y. Wu, "Unknown object retrieval in confined space through reinforcement learning with tactile exploration," in *Proc. IEEE Int. Conf. Robot. Automat.*, 2024, pp. 10881–10887.

[6] P. Avhad, G. P. Kumar, A. T. Sunil, M. Rallapalli, B. H. Kumar, and V. Kumar, "Adaptive deep reinforcement learning for robotic manipulation in dynamic environments," in *Proc. Int. Conf. Data Sci. Netw. Secur.*, 2024, pp. 1–5.

[7] G. Zhang, B. Wang, K. Liu, B. Pei, and C. Feng, "A deep reinforcement learning-based motion planner for human-robot collaboration in pathological experiments," in *Proc. IEEE 7th Inf. Technol. Mechatron. Eng. Conf.*, 2023, pp. 504–508.

[8] G. Li, X. Liang, Y. Gao, T. Su, Z. Liu, and Z.-G. Hou, "A linkage-driven underactuated robotic hand for adaptive grasping and in-hand manipulation," *IEEE Trans. Automat. Sci. Eng.*, vol. 21, no. 3, pp. 3039–3051, Jul. 2024.

[9] K. Yamaguchi, Y. Hirata, and K. Kosuge, "Underactuated robot hand for dual-arm manipulation," in *Proc. IEEE/RSJ Int. Conf. Intell. Robots Syst.*, 2015, pp. 2937–2942.

[10] Y. Kita, F. Kanehiro, T. Ueshiba, and N. Kita, "Clothes handling based on recognition by strategic observation," in *Proc. 11th IEEE-RAS Int. Conf. Humanoid Robots*, 2011, pp. 53–58.

[11] Y. Koishihara, S. Arnold, K. Yamazaki, and T. Matsubara, "Hanging work of T-shirt in consideration of deformability and stretchability," in *Proc. IEEE Int. Conf. Inf. Automat.*, 2017, pp. 130–135.

[12] A. Ramisa, G. Alenyà, F. Moreno-Noguer, and C. Torras, "Using depth and appearance features for informed robot grasping of highly wrinkled clothes," in *Proc. IEEE Int. Conf. Robot. Automat.*, 2012, pp. 1703–1708.

[13] K. S. M. Sahari, H. Seki, Y. Kamiya, and M. Hikizu, "Edge tracing manipulation of clothes based on different gripper types," *J. Comput. Sci.*, vol. 6, no. 8, pp. 872–879, Aug. 2010.

[14] P. N. Koustoumpardis, K. X. Nastos, and N. A. Aspragathos, "Underactuated 3-finger robotic gripper for grasping fabrics," in *Proc. 23rd Int. Conf. Robot. Alpe-Adria-Danube Region*, 2014, pp. 1–8.

[15] A. Doumanoglou et al., "Folding clothes autonomously: A complete pipeline," *IEEE Trans. Robot.*, vol. 32, no. 6, pp. 1461–1478, Dec. 2016.

[16] X. Chen, J. V. Salazar Luces, A. E. Petrilli Barceló, and Y. Hirata, "A novel under-actuated robotic hand for production tasks," in *Proc. IEEE Int. Conf. Robot. Biomimetics*, 2023, pp. 1–7.

[17] J. Borràs, G. Alenyà, and C. Torras, "A grasping-centered analysis for cloth manipulation," *IEEE Trans. Robot.*, vol. 36, no. 3, pp. 924–936, Jun. 2020.

[18] P. Jimenez, "Visual grasp point localization, classification and state recognition in robotic manipulation of cloth: An overview," *Robot. Auton. Syst.*, vol. 92, pp. 107–125, 2017.

[19] J. Maitin-Shepard, M. Cusumano-Towner, J. Lei, and P. Abbeel, "Cloth grasp point detection based on multiple-view geometric cues with application to robotic towel folding," in *Proc. IEEE Int. Conf. Robot. Automat.*, 2010, pp. 2308–2315.

[20] M. Shibata and S. Hirai, "Fabric manipulation utilizing contacts with the environment," in *Proc. IEEE Int. Conf. Automat. Sci. Eng.*, 2012, pp. 442–447.

[21] B. Sun and X. Zhang, "A new electrostatic gripper for flexible handling of fabrics in automated garment manufacturing," in *Proc. IEEE 15th Int. Conf. Automat. Sci. Eng.*, 2019, pp. 879–884.

[22] S. Marullo, S. Bartoccini, G. Salvietti, M. Z. Iqbal, and D. Prattichizzo, "The Mag-Gripper: A soft-rigid gripper augmented with an electromagnet to precisely handle clothes," *IEEE Robot. Automat. Lett.*, vol. 5, no. 4, pp. 6591–6598, Oct. 2020.